Hydrothermal carbonization of olive wastes to produce renewable, binder-free pellets for use as metallurgical reducing agents

Gerrit Ralf Surup[a], James J. Leahy[b], Michael T Timko[c], Anna Trubetskaya[b,*]

[a] *Department of Materials Science and Engineering, Norwegian University of Science and Technology, 7491, Trondheim, Norway*
[b] *Bernal Center, University of Limerick, Castletroy, Ireland*
[c] *Chemical Engineering Department, Worcester Polytechnic Institute, 01609 Worcester, MA, USA*

S-1. Hydrochar composition

The proximate analysis, ultimate analysis and calorific values of olive pulp hydrochar are summarized in Table S-1.

*Corresponding author email: anna.trubetskaya@ul.ie

Table S-1: Yield and composition of products from stirred hydrothermal carbonization.

	Product yield			Proximate analysis			Ultimate analysis					
Temperature	Solid	Liquid	Gases	VM	FC	ash	C	H	N	S	O	HHV
°C		wt.%					%					MJ kg^{-1}
residence time = 2 h												
200	65.3	28.3	5.8	66.9	31.6	1.5	57.7	6.6	1.0	0.1	33.1	23.99
220	60.4	30.9	7.7	63.2	34.7	2.1	60.8	7.2	1.1	0.1	28.7	25.11
240	51.6	38.4	10.3	55.1	42.9	2.0	67.7	7.0	1.0	0.1	22.2	27.86
Residence time = 6 h												
190	61.0	18.2	4.8	63.1	34.8	2.1	60.1	6.1	1.2	0.1	30.5	23.95
200	54.6	26.5	9.2	55.6	42.3	2.1	65.1	7.2	1.3	0.2	24.1	26.85
210	43.7	36.2	8.4	57.3	40.6	2.1	63.3	5.9	1.3	0.1	27.3	25.59
220	40.6	37.4	8.9	53.6	43.3	3.1	66.9	6.0	1.3	0.1	22.6	27.52
230	39.5	38.2	9.9	50.5	47.4	2.1	69.1	5.9	1.5	0.1	21.3	28.90
240	37.2	38.6	10.3	49.4	48.5	2.1	70.2	6.1	1.3	0.1	20.2	29.11
250	34.1	41.3	10.6	48.2	49.8	2.0	71.5	5.9	1.5	0.1	19.0	29.50
Residence time = 15 h												
190	63.3	27.3	8.5	61.5	36.7	1.8	61.6	7.5	1.2	0.1	27.8	24.45
200	61.9	26.4	7.7	63.8	34.0	2.2	60.6	7.2	1.2	0.2	28.6	24.53
210	52.2	34.4	10.7	51.7	46.0	2.3	66.9	6.0	1.4	0.1	23.3	28.03
220	49.1	35.4	12.5	48.5	48.6	2.9	68.9	7.0	1.5	0.2	19.6	28.36
230	48.4	33.4	11.8	48.2	49.8	2.0	70.0	6.7	1.5	0.1	19.7	28.21
240	45.6	30.9	13.3	46.4	50.7	2.9	71.3	7.3	1.5	0.1	16.9	29.42
250	43.7	29.6	13.0	41.8	56.2	2.0	70.4	6.1	1.6	0.1	19.8	28.79

The solid yield and volatile matter of olive pulp reacted at low heat treatment temperatures are shown in Figure S-1.

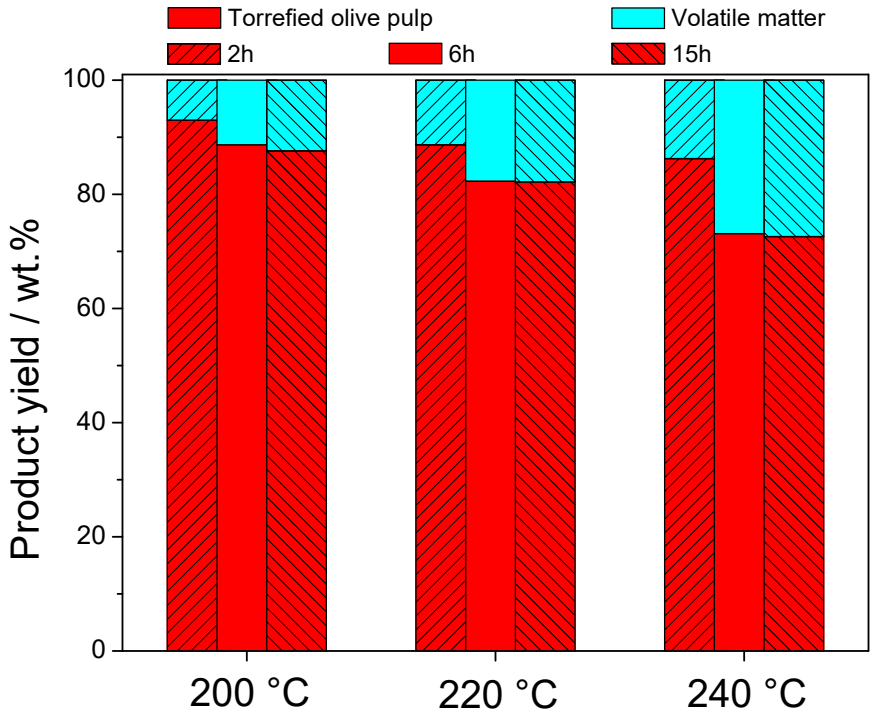

Figure S-1: Solid yield and volatile matter of olive pulp reacted in the TGA at 200, 220 and 240°C and after 2, 6 and 15 h.

S-2. FTIR analysis

FTIR spectra of olive pulp and hydrochar produced at 190, 220 and 250°C are summarized in Table S-2.

Table S-2: Summary of FT-IR peak/band assignment for olive pulp and the hydrochar generated at 190, 220 and 250°C.

Band position, cm^{-1}							Peak assignment
Original	Olive pulp	190°C, 6 h	220°C, 6 h	250°C, 6 h	250°C, 15 h	250°C, 60 h	
3200-3600	3492		3425	3510		3513	O-H stretch [1–3]
3100-3488	3253		3279	3327			O-H stretch [1, 2]
2942	2918	2921	2921	2918	2925	2917	C-H stretch [1]
	2840	2851	2858	2854	2854	2854	C-H stretch [1]
				1781	1784	1781	C-H stretch [4]
		1703	1700	1696	1697	1699	aromatic stretch [4]
1635	1636						N-H plane bonding [2]
1589		1599	1592	1591	1591	1587	C=C stretch [2]
1500-1550	1516	1513	1505	1501	1509	1509	aromatic stretch [4]
1442,1449	1445	1457	1442	1442	1445	1442	C=C stretch vs(ν) [5]
1374	1378	1371					C-H bending [3]
1363			1360	1360	1371	1360	In-the-plane C-H bending [3]
1321	1319	1315					COH stretch
1259		1271	1260	1260	1274	1259	G ring stretching [3]
1232	1233						COH bending at C6
1204		1211	1211	1206	1200	1203	C-O-C symmetric stretching
							O-H plane deformation [3]
	1136	1157					C-O stretch
1098, 1103		1110	1104	1097	1099	1091	C-O stretch, -OCH_3 [5, 6]
1020	1047	1025	1018	1017	1021	1009	C-C, C-OH, C-H ring
							side group vibrations [3]
994	998						C-C, C-OH, C-H ring
							side group vibrations [3]
	927	917	927	950	946	935	C-O stretch
	819	804	804	801	801	798	C-O stretch
662		734	667				C-OH out-of-plane bending [3]

S-3. Reactivity

Figure S-2 shows differential weight loss curves (DTG) for 100 % volume fraction CO_2 gasification of olive pulp samples reacted at low heat treatment temperatures.

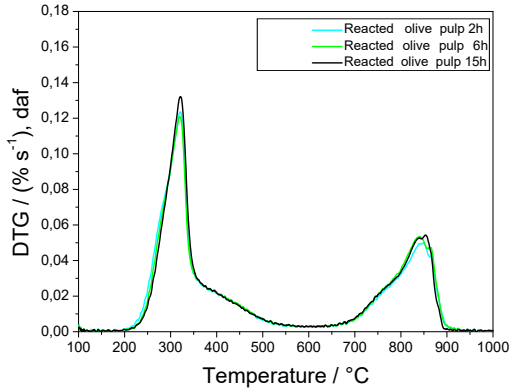

2(a): 200 °C

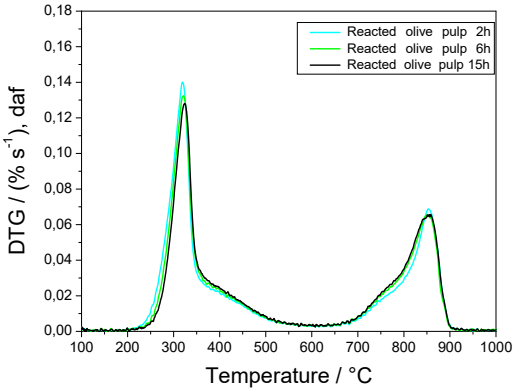

2(b): 220 °C

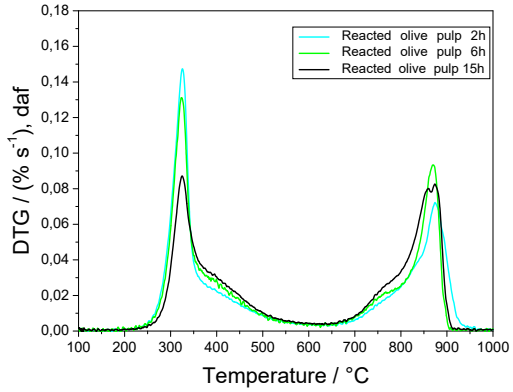

2(c): 240 °C

Figure S-2: DTG curves of olive pulp reacted in 100 % volume fraction CO_2 from pyrolysis at: (a) 200°C, (b) 220°C and (c) 240°C and after 2, 6 and 15 h.

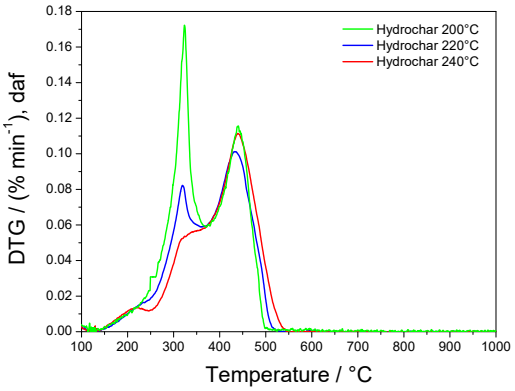

3(a): Air 2 h

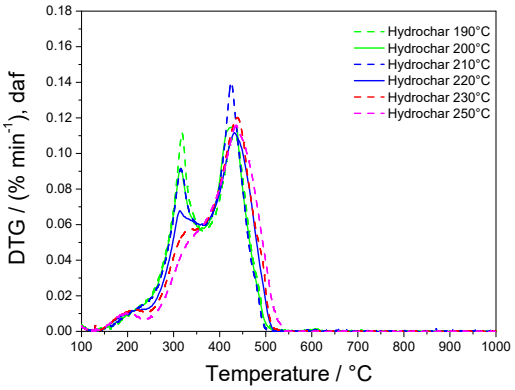

3(b): Air 6 h

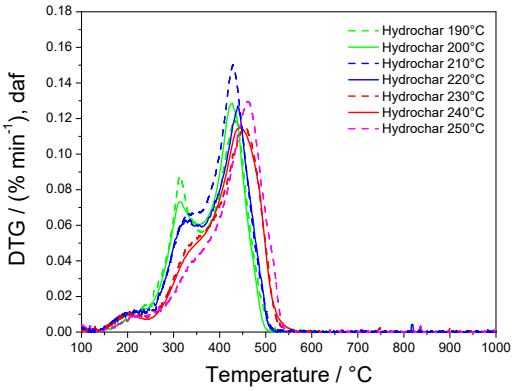

3(c): Air 15 h

Figure S-3: DTG curves of olive pulp oxidation after torrefaction: (a) at 200, 220 and 240°C in the TGA and hydrothermal carbonization at 190, 200, 210, 220, 230 and 250°C after (b) 6 h and (c) 15 h.

The peak temperature of low temperature reacted olive pulp ranged from 650 to 900°C, whereas the maximum reaction rate shifted from 845 to 867°C with the increase in heat treatment temperature of olive pulp. Figure S-3 shows differential weight loss curves (DTG) in 100 % air. All samples were fully oxidized at 550°C, whereas the reactivity slightly decreased with the increased heat treatment temperature from 435 to 450°C. The Arrhenius plots of hydrochar oxidation reactivity are shown in Figure S-4.

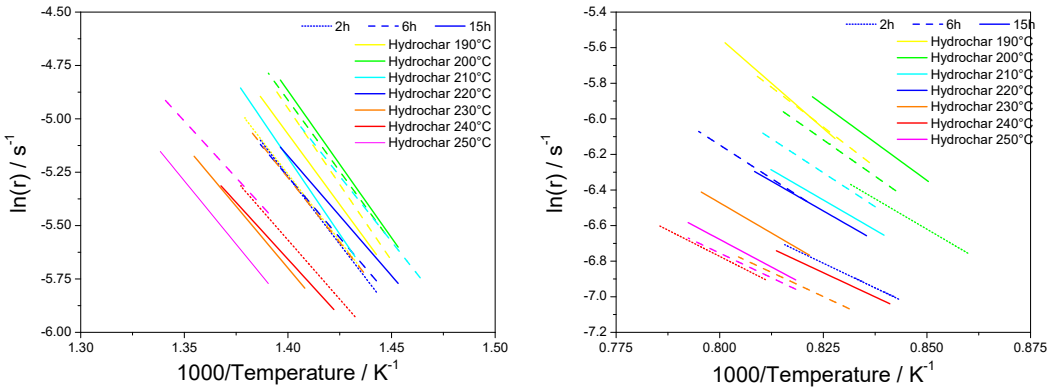

4(a): CO_2 4(b): air

Figure S-4: Arrhenius plot of reactivity of hydrochar from HTC treatment in the temperature range 190 to 250°C in 100 % volume fraction CO_2 and in air.

S-4. Discussion

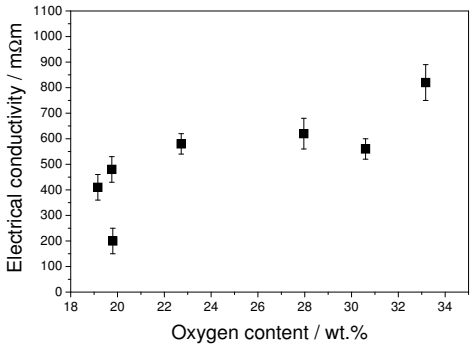

5(a): Electrical resistivity

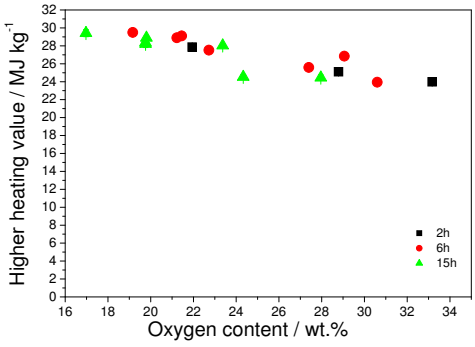

5(b): Higher heating value

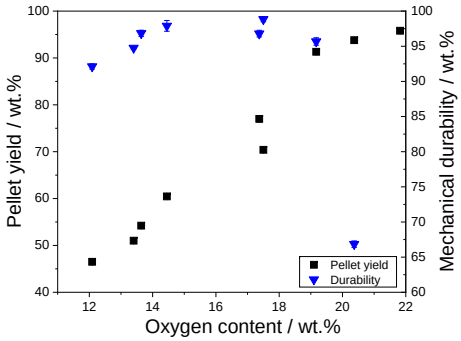

5(c): Pellet yield and mechanical durability

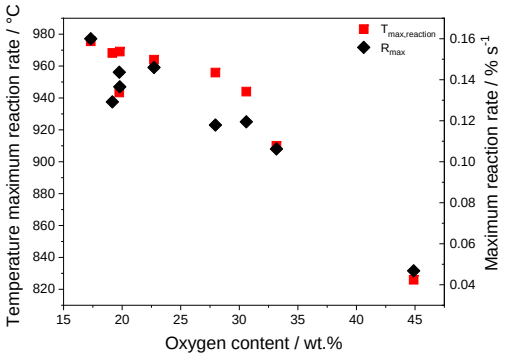

5(d): Reactivity

Figure S-5: Correlations of electrical resistivity, higher heating value, pellet yield, mechanical durability, maximum reaction rate and temperature of maximum reaction rate over oxygen content of hydrochar from olive pulp treatment produced at 190, 220 and 250°C with a residence time of 6 h, olive pulp hydrochar generated at 250°C with a residence time of 6, 15 and 60 h and olive pulp hydrochar prepared at 250°C with a residence time of 6 h further reacted in the range from 300 to 1100°C in a high-temperature furnace.

References

References

[1] Arellano O, Flores M, Guerra J, Hidalgo A, Rojas D, Strubinger A, Hydrothermal Carbonization of Corncob and Characterization of the Obtained Hydrochar, Chem Eng Trans 50 (2016) 235–40.

[2] El-Hendawy ANA, Variation in the FTIR spectra of a biomass under impregnation, carbonization and oxidation conditions, J Anal Appl Pyrolysis 75 (2004) 159–66.

[3] Fan M, Dai D, Huang B, Chapter 3 Fourier Transform Infrared Spectroscopy for Natural Fibres. In (ed. Salih SM): Fourier Transform, IntechOpen (2012) 45–68.

[4] Adapa PK, Tabil LG, Schoenau GJ, Canam T, Dumonceaux T, Quantitative Analysis of Lignocellulosic Components of Non-Treated and Steam Exploded Barley, Canola, Oat and Wheat Straw Using Fourier Transform Infrared Spectroscopy, J Agr Sci Tech B 1 (2011) 177–88.

[5] Liu Z, Quek A, Hoekman SK, Balasubramanian R, Production of solid biochar fuel from waste biomass by hydrothermal carbonization, Fuel 103 (2013) 943–9.

[6] Arafat A, Samad SA, Masum SM, Moniruzzaman M, Preparation and Characterization of Chitosan from Shrimp shell waste, IJSER 6 (5) (2015) 538–41.